

Supplement of Biogeosciences Discuss., 11, 10323–10363, 2014  
<http://www.biogeosciences-discuss.net/11/10323/2014/>  
doi:10.5194/bgd-11-10323-2014-supplement  
© Author(s) 2014. CC Attribution 3.0 License.



*Supplement of*

## **On the relationship between ecosystem-scale hyperspectral reflectance and CO<sub>2</sub> exchange in European mountain grasslands**

**M. Balzarolo et al.**

*Correspondence to:* M. Balzarolo (manunela.balzarolo@uantwerpen.be)

Supplementary Material

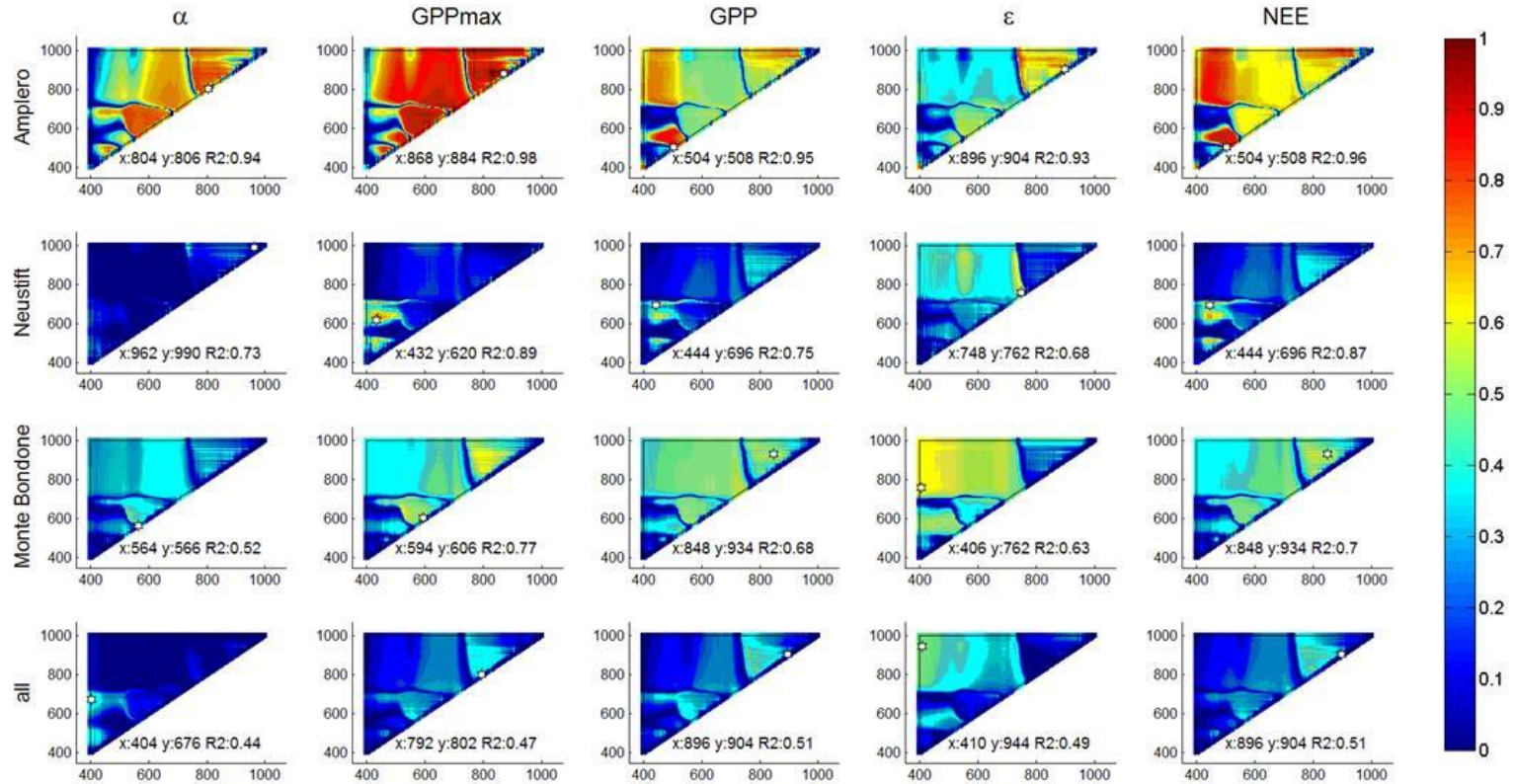


Figure S1. Correlograms of  $R^2$  values for  $\alpha$ ,  $GPP_{max}$  and midday averaged GPP,  $\epsilon$  and NEE and NSD-type indices for Amplero, Neustift, Monte Bondone (both study years pooled) and all sites pooled for the linear model. The asterisks indicate the position of paired band combinations corresponding to the maximum  $R^2$ . The masked correlograms are shown in Figure 4.

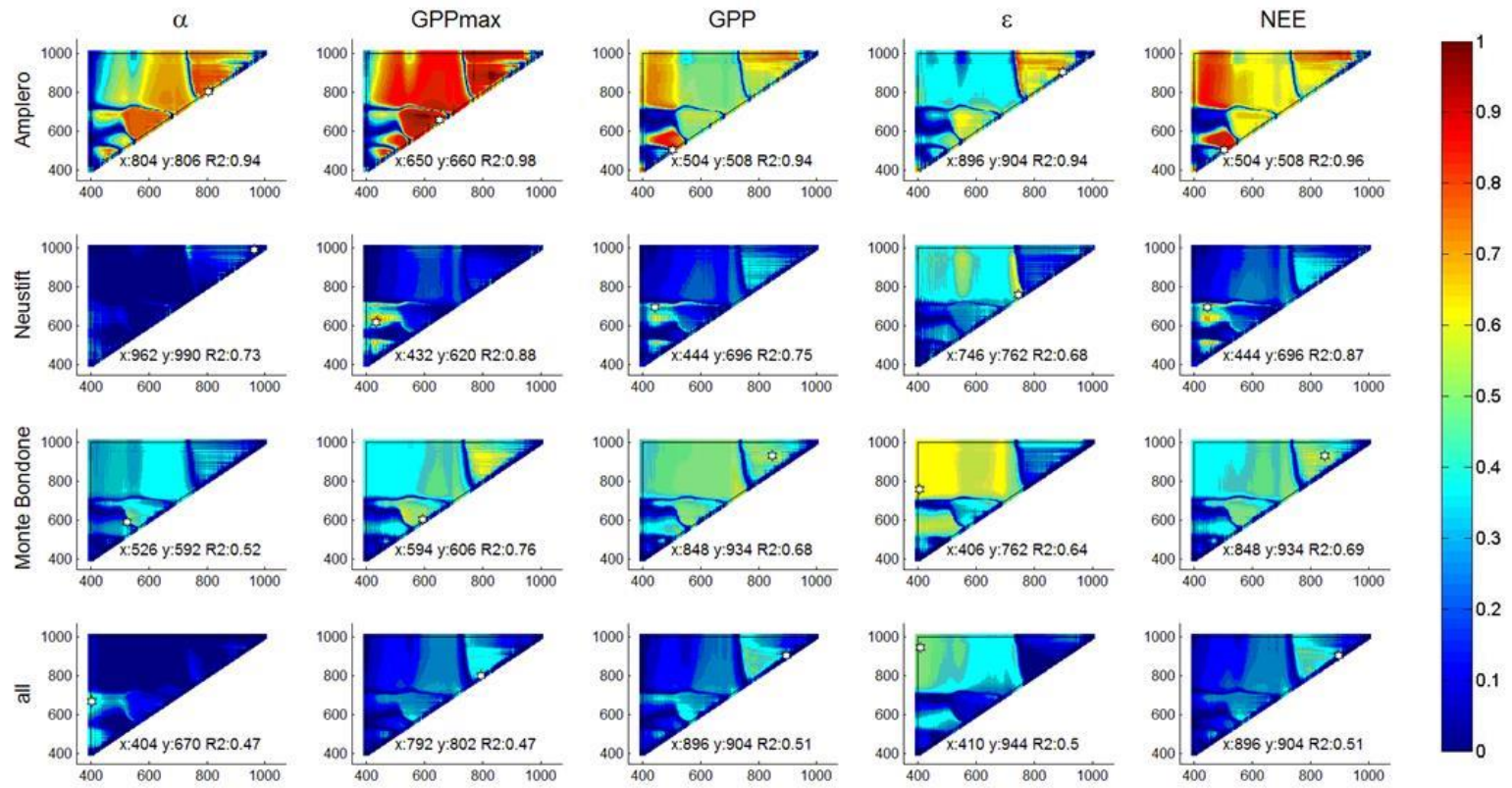


Figure S2. Correlograms of  $R^2$  values for  $\alpha$ ,  $GPP_{max}$  and midday averaged GPP,  $\epsilon$  and NEE and SR-type indices for Amplero, Neustift, Monte Bondone (both study years pooled) and all sites pooled for the linear model. The asterisks indicate the position of paired band combinations corresponding to the maximum  $R^2$ . The masked correlograms are shown in Figure 5.

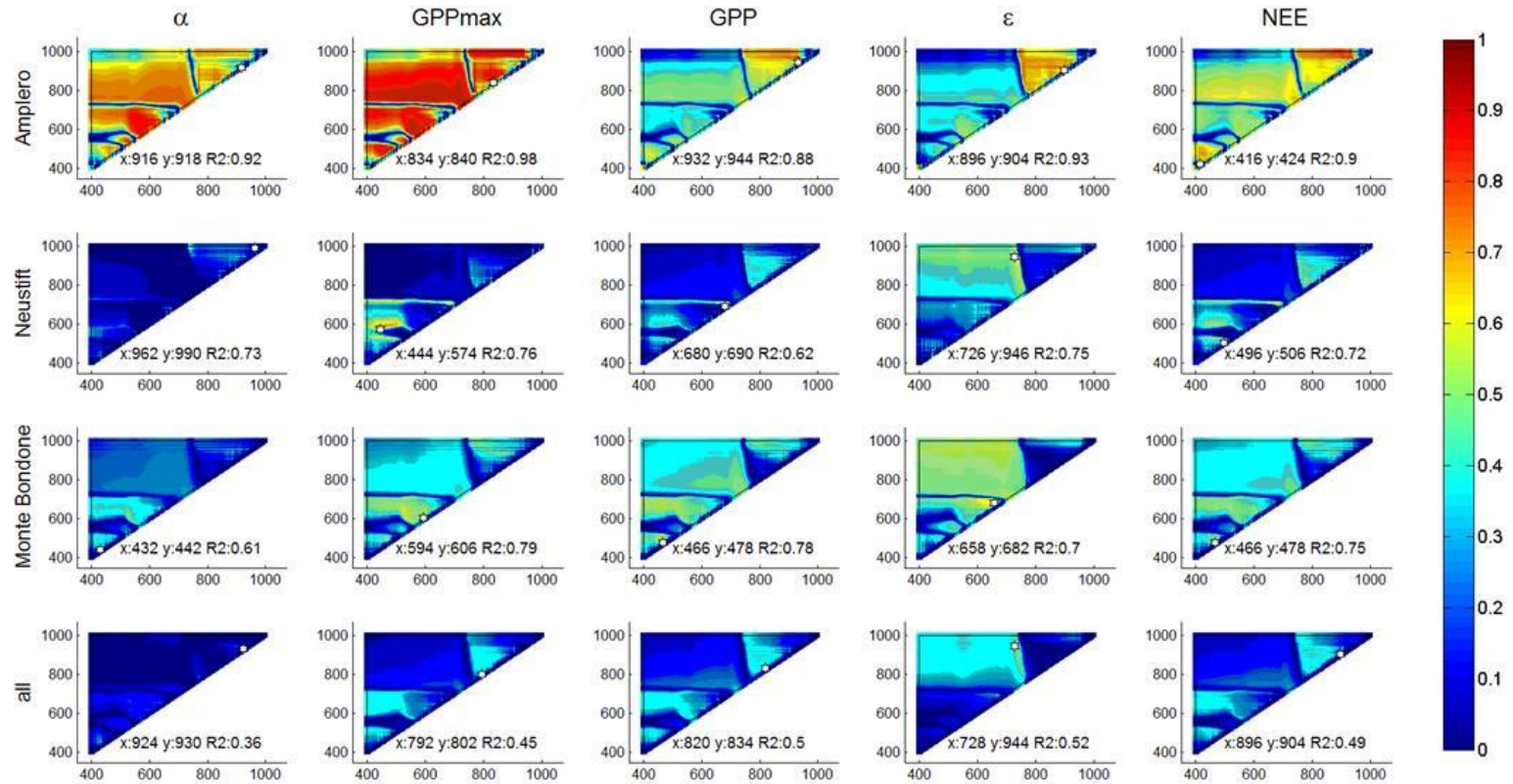


Figure S3. Correlograms of  $R^2$  values for  $\alpha$ ,  $GPP_{max}$  and midday averaged GPP,  $\epsilon$  and NEE and SD-type indices for Amplero, Neustift, Monte Bondone (both study years pooled) and all sites pooled for the linear model. The asterisks indicate the position of paired band combinations corresponding to the maximum  $R^2$ . The masked correlograms are shown in Figure 6.



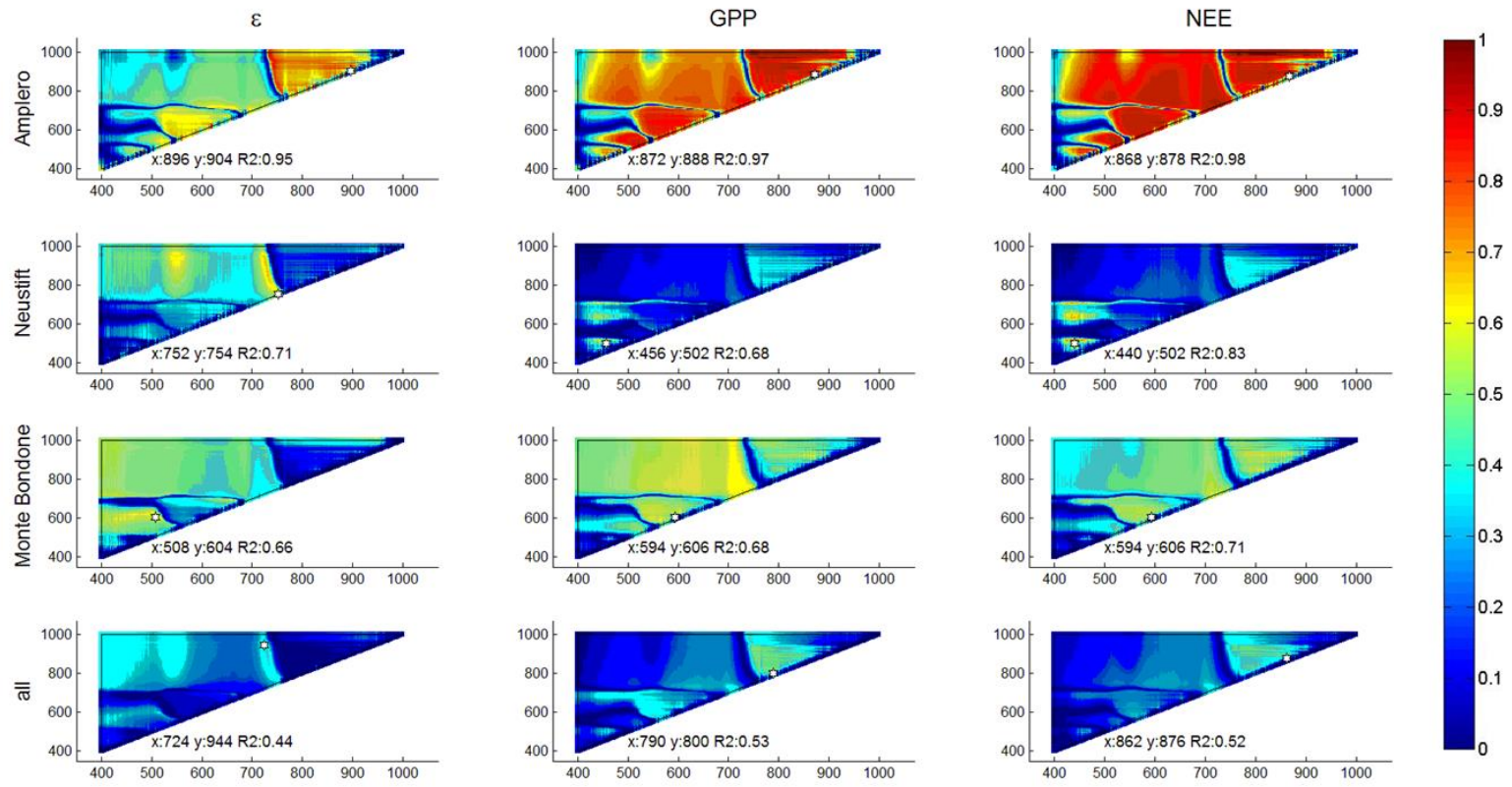


Figure S4. Correlograms of  $R^2$  values for daily averaged GPP,  $\epsilon$  and NEE and NSD-type indices for Amplero, Neustift, Monte Bondone (both study years pooled) and all sites pooled for the linear model. The asterisks indicate the position of paired band combinations corresponding to the maximum  $R^2$ .

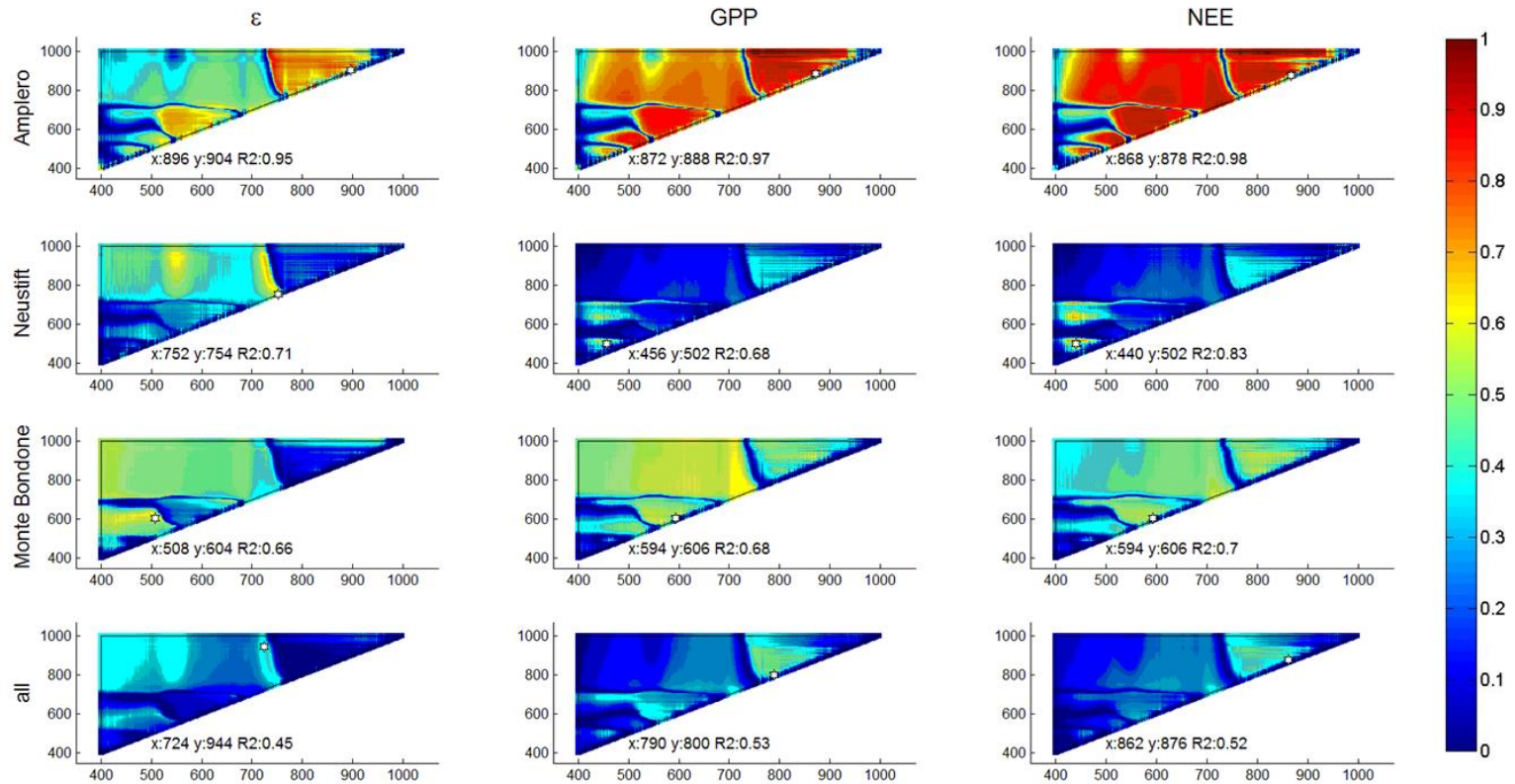


Figure S5. Correlograms of  $R^2$  values for daily averaged GPP,  $\epsilon$  and NEE and SR-type indices for Amplero, Neustift, Monte Bondone (both study years pooled) and all sites pooled for the linear model. The asterisks indicate the position of paired band combinations corresponding to the maximum  $R^2$ .

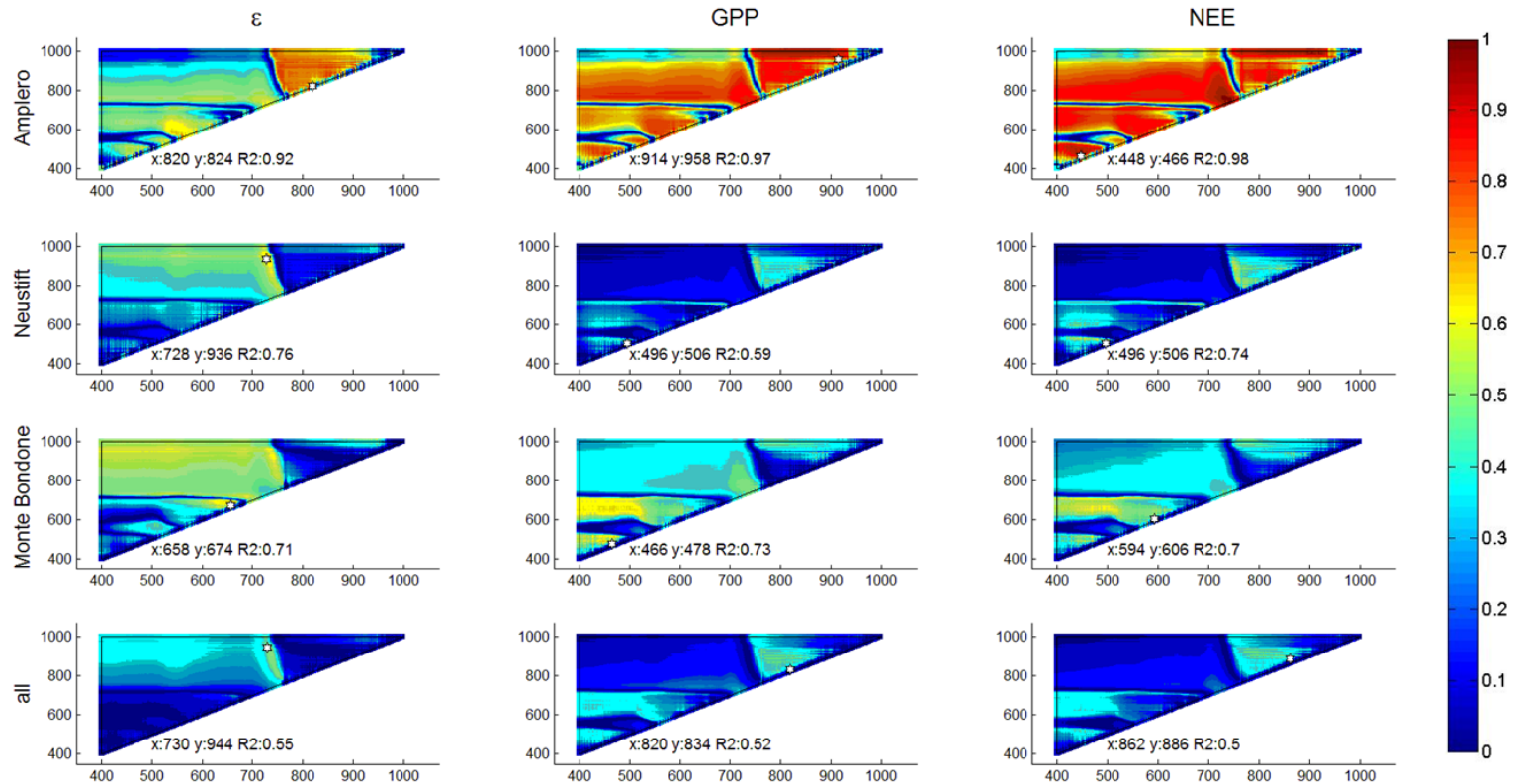


Figure S6. Correlograms of  $R^2$  values for daily averaged GPP,  $\epsilon$  and NEE and SD-type indices for Amplero, Neustift, Monte Bondone (both study years pooled) and all sites pooled for the linear model. The asterisks indicate the position of paired band combinations corresponding to the maximum  $R^2$ .

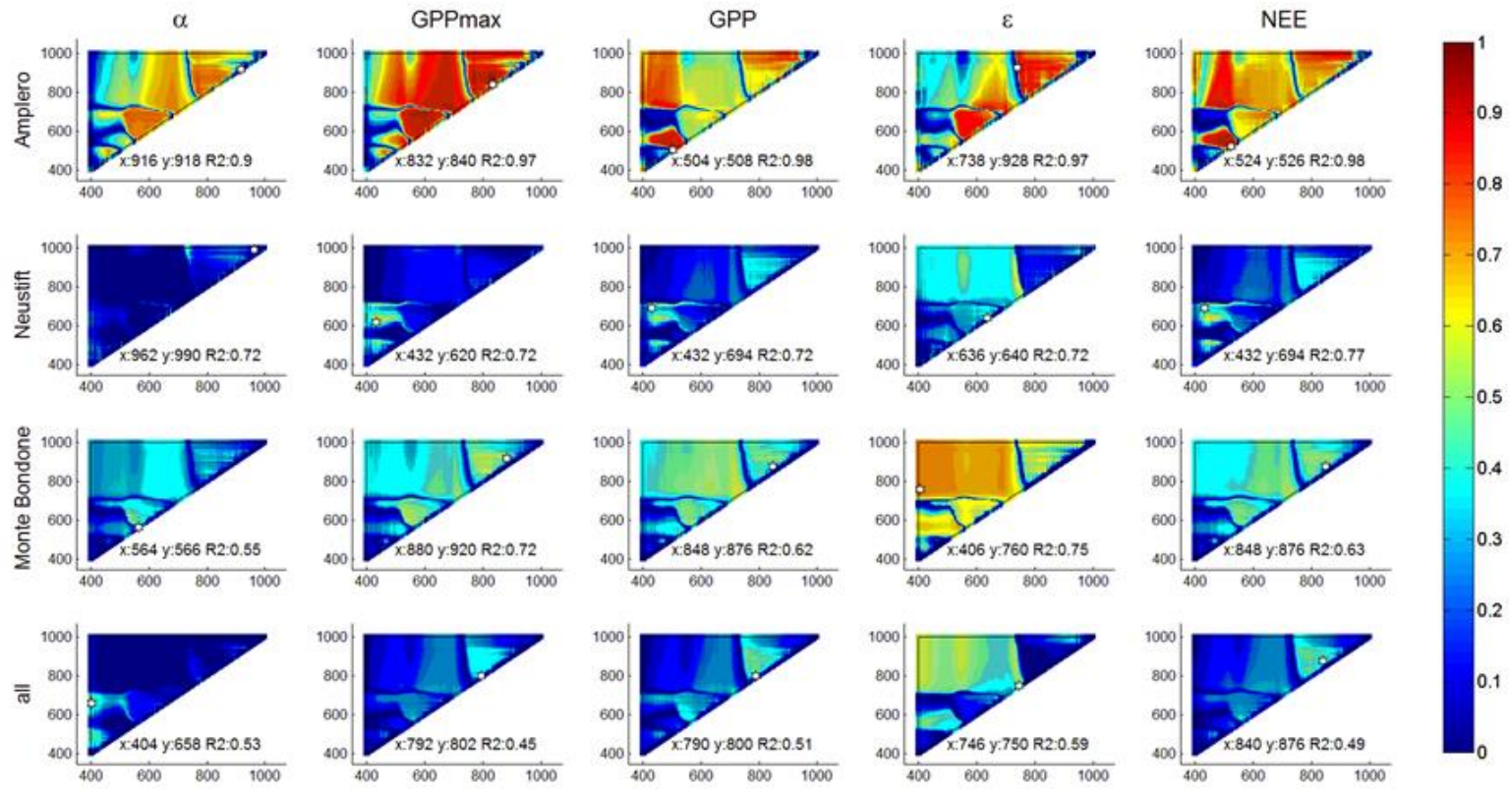


Figure S7. Correlograms of  $R^2$  values for  $\alpha$ ,  $GPP_{\max}$  and midday averaged GPP,  $\epsilon$  and NEE and NSD-type indices for Amplero, Neustift, Monte Bondone (both study years pooled) and all sites pooled for the exponential model. The asterisks indicate the position of paired band combinations corresponding to the maximum  $R^2$ . The masked correlograms are shown in Figure 7.



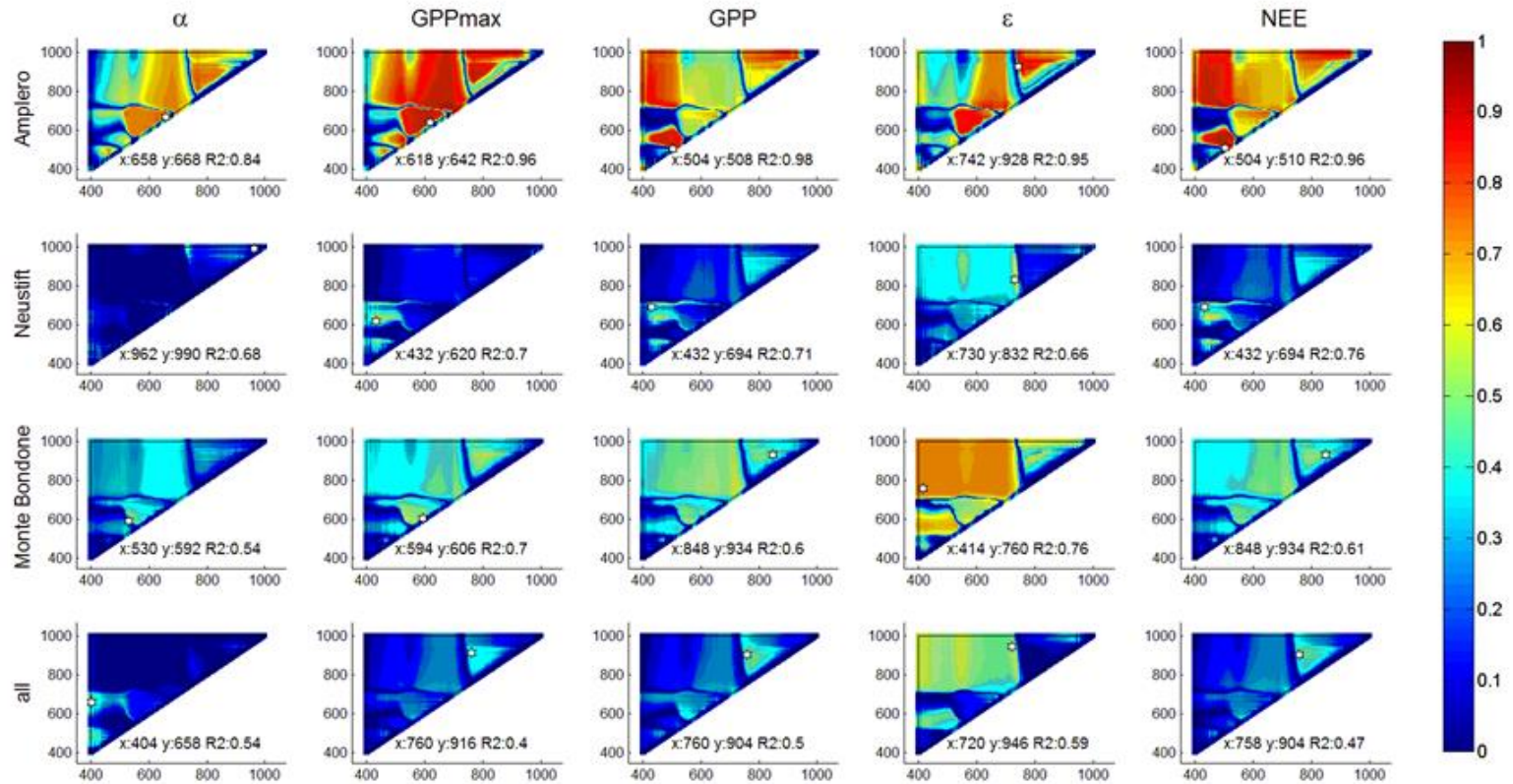


Figure S8. Correlograms of  $R^2$  values for  $\alpha$ ,  $GPP_{max}$  and midday averaged GPP,  $\epsilon$  and NEE and SR-type indices for Amplero, Neustift, Monte Bondone (both study years pooled) and all sites pooled for the exponential model. The asterisks indicate the position of paired band combinations corresponding to the maximum  $R^2$ . The masked correlograms are shown in Figure 8.

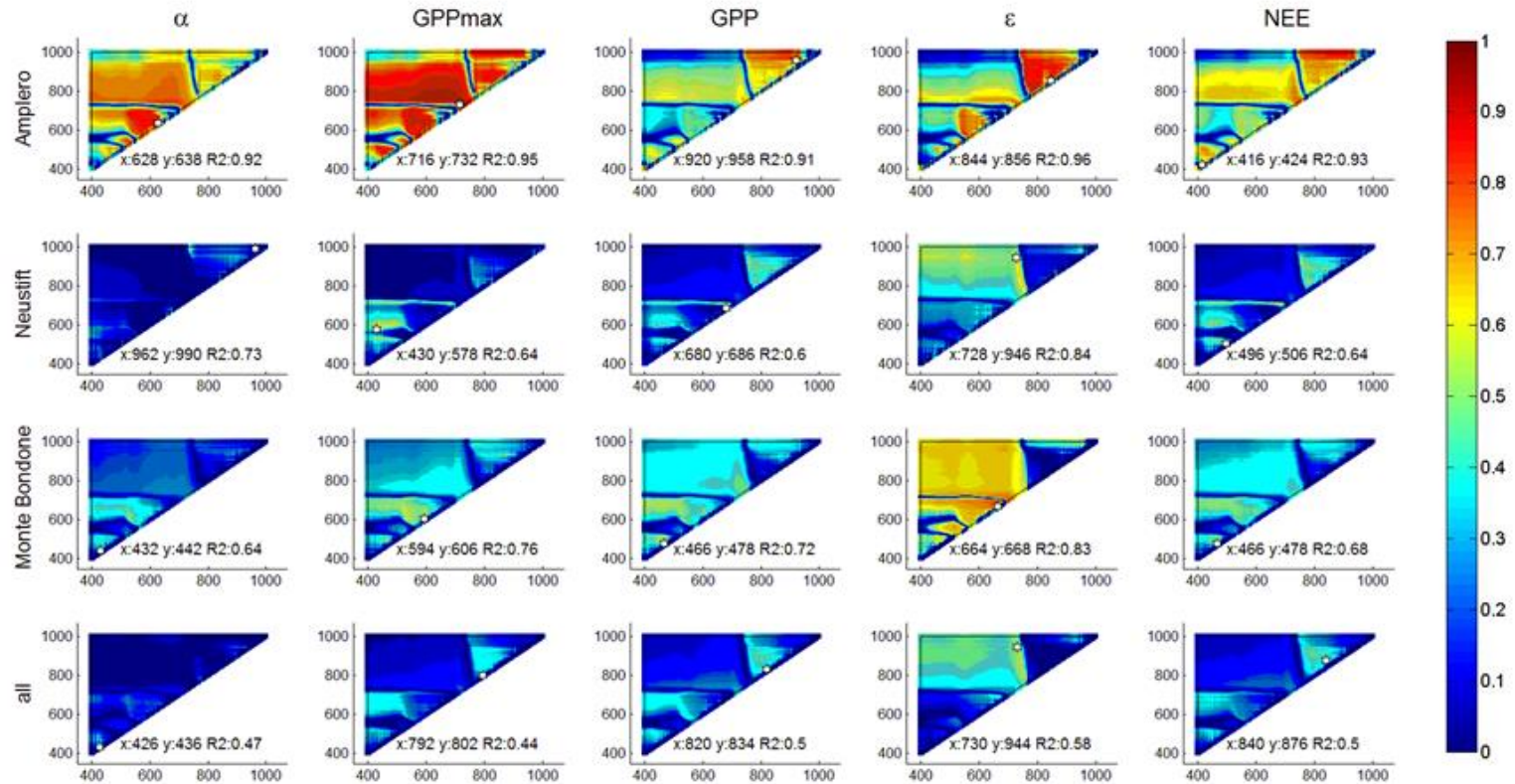


Figure S9. Correlograms of  $R^2$  values for  $\alpha$ ,  $GPP_{max}$  and midday averaged GPP,  $\epsilon$  and NEE and SD-type indices for Amplero, Neustift, Monte Bondone (both study years pooled) and all sites pooled for the exponential model. The asterisks indicate the position of paired band combinations corresponding to the maximum  $R^2$ . The masked correlograms are shown in Figure 9.

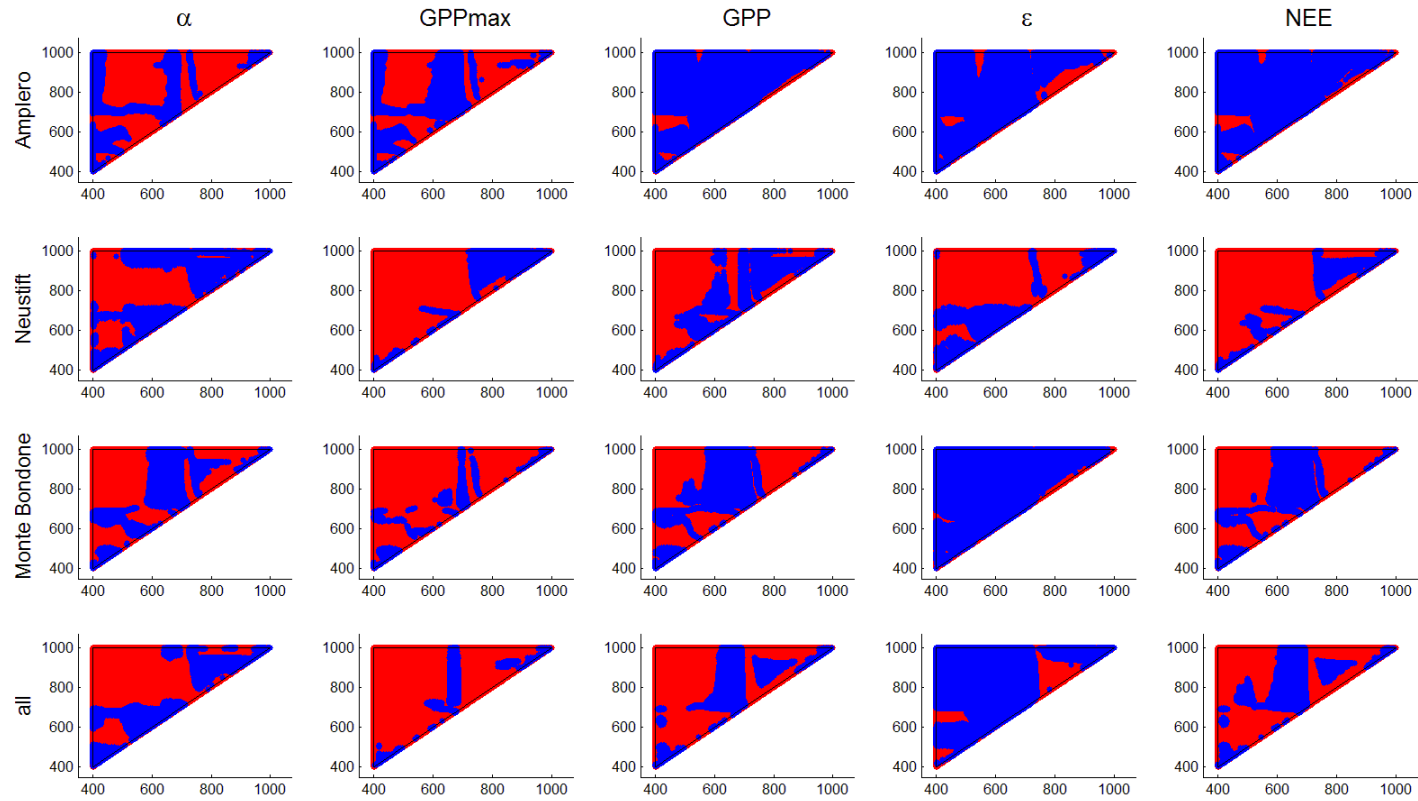


Figure S10. Correlograms of the differences between AIC (Akaike information criterion) obtained for linear and exponential models for  $\alpha$ ,  $GPP_{\max}$  and midday averaged GPP,  $\epsilon$  and NEE and SR-type indices for Amplero, Neustift, Monte Bondone (both study years pooled) and all sites pooled. Red areas indicate waveband combinations where the linear model performed better than exponential one, while blue areas indicate the reverse.

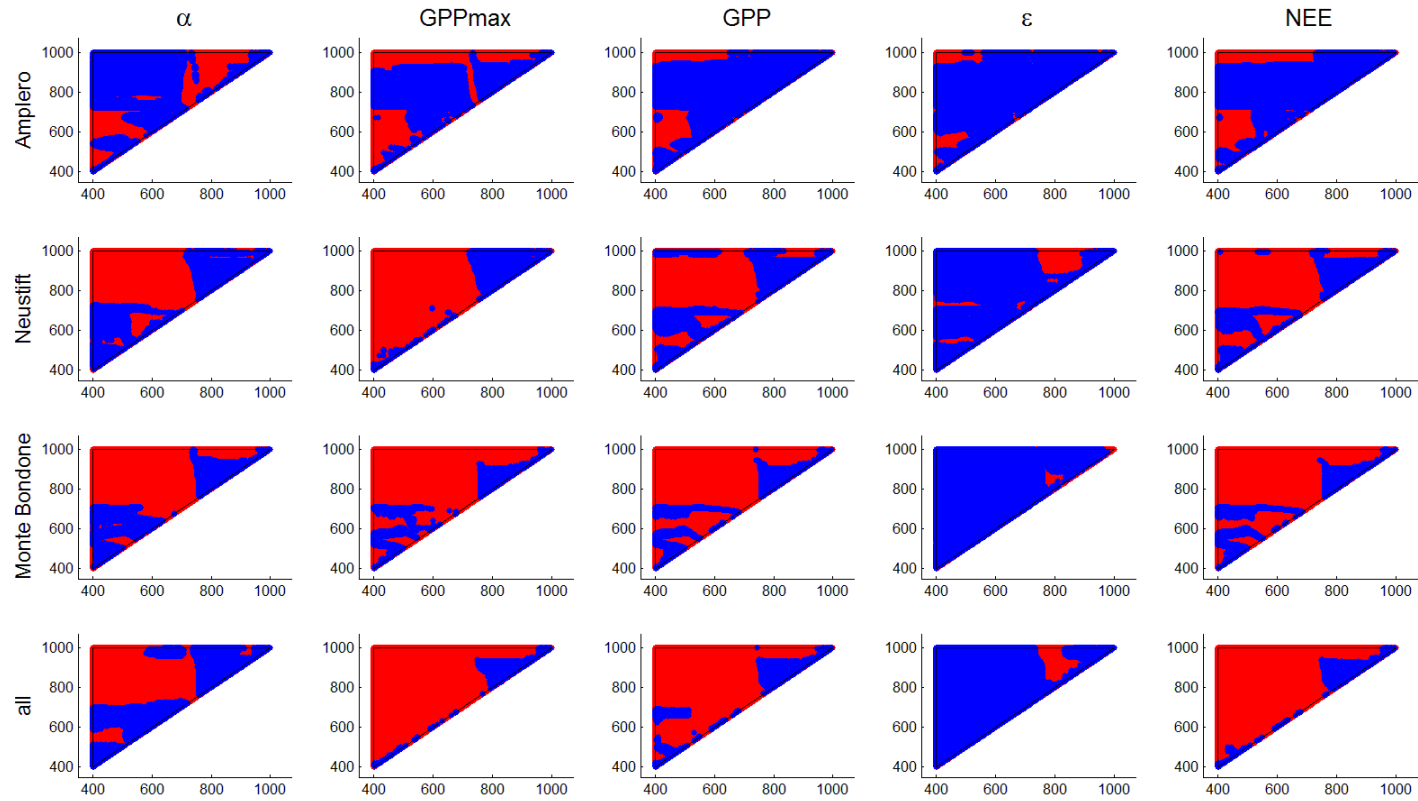


Figure S11. Correlograms of the differences between AIC (Akaike information criterion) obtained for linear and exponential models for  $\alpha$ ,  $GPP_{max}$  and midday averaged GPP,  $\epsilon$  and NEE and SD-type indices for Amplero, Neustift, Monte Bondone (both study years pooled) and all sites pooled. Red areas indicate waveband combinations where the linear model performed better than exponential one, while blue areas indicate the reverse.



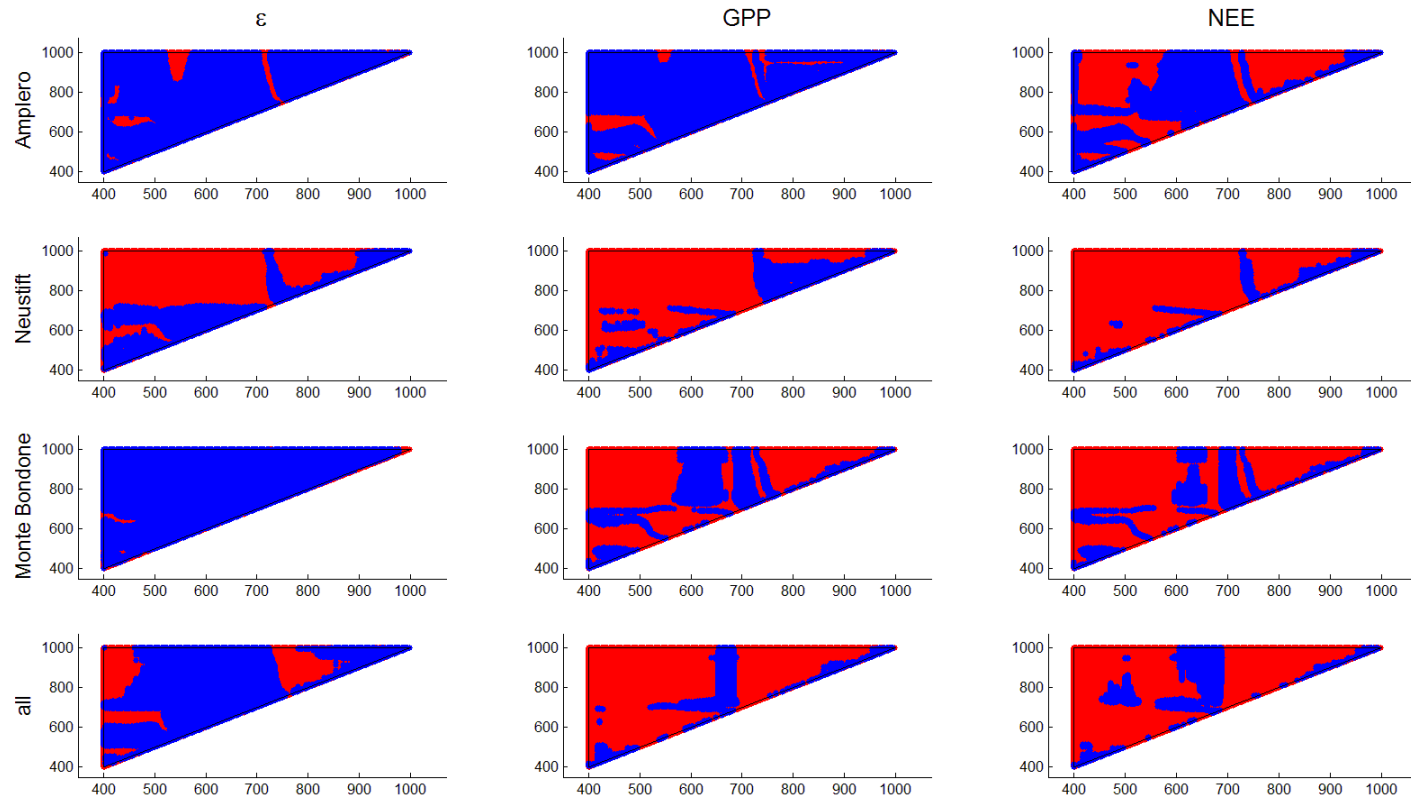


Figure S12. Correlograms of the differences between AIC (Akaike information criterion) obtained for linear and exponential models for daily averaged GPP,  $\varepsilon$  and NEE and NSD-type indices for Amplero, Neustift, Monte Bondone (both study years pooled) and all sites pooled. Red areas indicate waveband combinations where the linear model performed better than exponential one, while blue areas indicate the reverse.

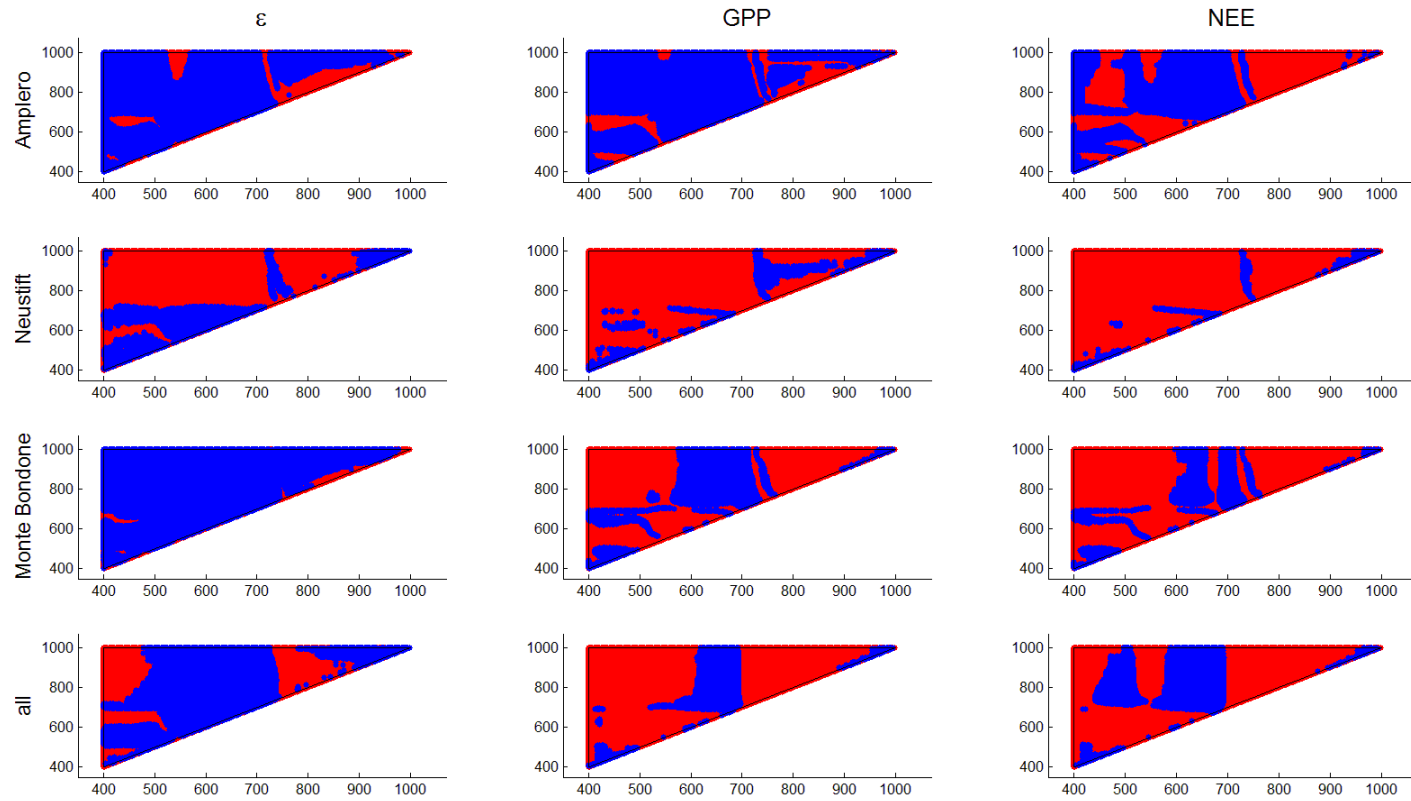


Figure S13. Correlograms of the differences between AIC (Akaike information criterion) obtained for linear and exponential models for daily averaged GPP,  $\epsilon$  and NEE and SR-type indices for Amplero, Neustift, Monte Bondone (both study years pooled) and all sites pooled. Red areas indicate waveband combinations where the linear model performed better than exponential one, while blue areas indicate the reverse.

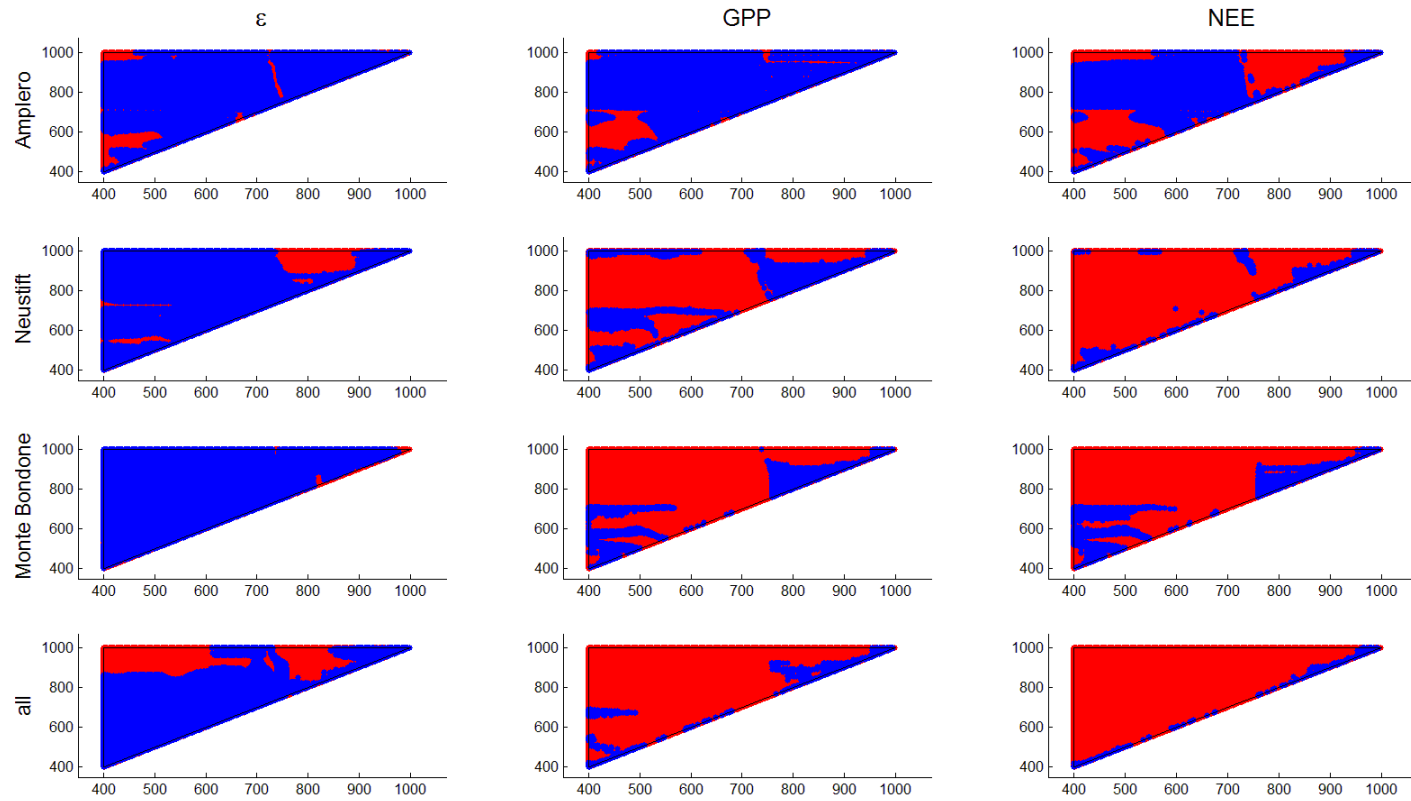


Figure S14. Correlograms of the differences between AIC (Akaike information criterion) obtained for linear and exponential models for daily averaged GPP,  $\varepsilon$  and NEE and SD-type indices for Amplero, Neustift, Monte Bondone (both study years pooled) and all sites pooled. Red areas indicate waveband combinations where the linear model performed better than exponential one, while blue areas indicate the reverse.

Table S1. Results of statistic of linear and exponential regression models between VIs and daily average of ecophysiological parameters:  $\epsilon$ , GPP and NEE.  $R^2$ —Coefficient of determination; RMSE—Root Mean Square Error; and AIC—Akaike information criterion. Bold letters indicate the best model between linear and exponential models. Dark grey shading highlights the model with the lowest AIC.

| VI                       | $\epsilon$  |            |            |   |            |            |   |            |             |  |            |             | GPP  |            |           |  |            |            |  |            |            |  |            |            | NEE  |            |           |  |            |           |  |            |            |  |            |            |  |
|--------------------------|---|------------|------------|---|------------|------------|---|------------|-------------|--|------------|-------------|--|------------|-----------|--|------------|------------|--|------------|------------|--|------------|------------|--|------------|-----------|--|------------|-----------|--|------------|------------|--|------------|------------|--|
|                          | Amplero   |            |            | Neustift  |            |            | Monte Bondone   |            |             | All  |            |             | Amplero  |            |           | Neustift   |            |            | Monte Bondone  |            |            | All  |            |            | Amplero  |            |           | Neustift   |            |           | Monte Bondone  |            |            | All  |            |            |  |
|                          | $R^2$   | RMSE       | AIC        | $R^2$   | RMSE       | AIC        | $R^2$   | RMSE       | AIC         | $R^2$  | RMSE       | AIC         | $R^2$  | RMSE       | AIC       | $R^2$  | RMSE       | AIC        | $R^2$  | RMSE       | AIC        | $R^2$  | RMSE       | AIC        | $R^2$  | RMSE       | AIC       | $R^2$  | RMSE       | AIC       | $R^2$  | RMSE       | AIC        | $R^2$  | RMSE       | AIC        |  |
|                          | $\frac{\mu\text{mol}_{\text{CO}_2}}{\mu\text{mol}_{\text{phot}}}$ | -          | -          | $\frac{\mu\text{mol}_{\text{CO}_2}}{\mu\text{mol}_{\text{phot}}}$ | -          | -          | $\frac{\mu\text{mol}_{\text{CO}_2}}{\mu\text{mol}_{\text{phot}}}$ | -          | -           | $\frac{\mu\text{mol}_{\text{CO}_2}}{\text{m}^2\text{s}}$ | -          | -           | $\frac{\mu\text{mol}_{\text{CO}_2}}{\text{m}^2\text{s}}$ | -          | -         | $\frac{\mu\text{mol}_{\text{CO}_2}}{\text{m}^2\text{s}}$ | -          | -          | $\frac{\mu\text{mol}_{\text{CO}_2}}{\text{m}^2\text{s}}$ | -          | -          | $\frac{\mu\text{mol}_{\text{CO}_2}}{\text{m}^2\text{s}}$ | -          | -          | $\frac{\mu\text{mol}_{\text{CO}_2}}{\text{m}^2\text{s}}$ | -          | -         | $\frac{\mu\text{mol}_{\text{CO}_2}}{\text{m}^2\text{s}}$ | -          | -         | $\frac{\mu\text{mol}_{\text{CO}_2}}{\text{m}^2\text{s}}$ | -          | -          | $\frac{\mu\text{mol}_{\text{CO}_2}}{\text{m}^2\text{s}}$ | -          |            |  |
| <i>Linear model</i>      |   |            |            |   |            |            |   |            |             |  |            |             |  |            |           |  |            |            |  |            |            |  |            |            |  |            |           |  |            |           |  |            |            |  |            |            |  |
| SR                       | <b>0.7</b>  | <b>0.0</b> | <b>-64</b> | 0.4   | 0.0        | -52        | 0.3   | 0.0        | -101        | 0.2  | 0.0        | -192        | 0.9  | 1.0        | 28        | 0.1  | 6.2        | 106        | 0.5  | 2.6        | 121        | 0.2  | 4.8        | 324        | <b>0.9</b>   | <b>0.7</b> | <b>21</b> | 0.1  | 5.5        | 102       | 0.5  | 2.4        | 117        | 0.2  | 4.0        | 304        |  |
| GRI                      | 0.4   | 0.0        | -59        | <b>0.5</b>  | <b>0.0</b> | <b>-57</b> | 0.4   | 0.0        | -105        | <b>0.4</b>   | <b>0.0</b> | <b>-202</b> | 0.7  | 1.5        | 35        | 0.1  | 6.2        | 106        | 0.5  | 2.6        | 121        | 0.1  | 5.2        | 333        | 0.9  | 1.1        | 30        | 0.1  | 5.5        | 102       | 0.4  | 2.6        | 120        | 0.1  | 4.2        | 309        |  |
| WI                       | 0.6   | 0.0        | -62        | 0.2   | 0.1        | -48        | 0.4   | 0.0        | -102        | 0.2  | 0.0        | -194        | <b>0.9</b>   | <b>0.9</b> | <b>25</b> | 0.0  | 6.3        | 106        | 0.4  | 3.0        | 127        | 0.1  | 5.1        | 329        | 0.9  | 0.8        | 23        | 0.0  | 5.7        | 103       | 0.3  | 2.7        | 122        | 0.1  | 4.2        | 310        |  |
| NDVI                     | 0.5   | 0.0        | -60        | 0.4   | 0.0        | -53        | 0.5   | 0.0        | -106        | 0.2  | 0.0        | -196        | 0.8  | 1.4        | 33        | 0.2  | 6.1        | 105        | 0.6  | 2.5        | 120        | 0.3  | 4.7        | 322        | 0.9  | 1.0        | 27        | 0.2  | 5.3        | 101       | 0.5  | 2.4        | 117        | 0.2  | 3.9        | 303        |  |
| SIPI                     | 0.4   | 0.0        | -58        | 0.3   | 0.0        | -52        | <b>0.5</b>  | <b>0.0</b> | <b>-108</b> | 0.2  | 0.0        | -193        | 0.6  | 1.8        | 38        | 0.2  | 5.9        | 104        | 0.5  | 2.6        | 120        | 0.3  | 4.4        | 319        | 0.8  | 1.5        | 35        | 0.2  | 5.1        | 99        | 0.5  | 2.4        | 116        | 0.3  | 3.8        | 302        |  |
| CI                       | 0.5   | 0.0        | -61        | 0.4   | 0.0        | -54        | 0.4   | 0.0        | -103        | 0.2  | 0.0        | -196        | 0.8  | 1.2        | 31        | 0.2  | 5.8        | 104        | <b>0.6</b>   | <b>2.4</b> | <b>116</b> | 0.2  | 4.7        | 322        | 0.9  | 0.8        | 23        | 0.2  | 5.1        | 100       | <b>0.6</b>   | <b>2.2</b> | <b>113</b> | <b>0.3</b>   | <b>3.9</b> | <b>300</b> |  |
| PRI                      | 0.7   | 0.0        | -64        | 0.1   | 0.1        | -47        | 0.0   | 0.0        | -91         | 0.0  | 0.0        | -185        | 0.7  | 1.5        | 34        | 0.2  | 5.9        | 104        | 0.2  | 3.4        | 134        | 0.3  | 4.6        | 317        | 0.8  | 1.4        | 33        | 0.2  | 5.3        | 101       | 0.2  | 3.0        | 129        | 0.1  | 4.2        | 310        |  |
| EVI                      | 0.5   | 0.0        | -60        | 0.4   | 0.0        | -54        | 0.5   | 0.0        | -107        | 0.2  | 0.0        | -196        | 0.8  | 1.4        | 34        | 0.1  | 6.1        | 105        | 0.5  | 2.8        | 124        | 0.2  | 4.8        | 324        | 0.9  | 1.1        | 30        | 0.1  | 5.4        | 101       | 0.4  | 2.5        | 119        | 0.2  | 4.1        | 307        |  |
| NPQI                     | 0.0   | 0.0        | -55        | 0.0   | 0.1        | -45        | 0.3   | 0.0        | -100        | 0.1  | 0.0        | -193        | 0.3  | 2.5        | 44        | 0.1  | 6.3        | 106        | 0.1  | 3.6        | 137        | 0.1  | 5.2        | 333        | 0.3  | 2.6        | 45        | 0.1  | 5.5        | 102       | 0.1  | 3.1        | 130        | 0.0  | 4.5        | 318        |  |
| NPCI                     | 0.4   | 0.0        | -58        | 0.2   | 0.1        | -48        | 0.0   | 0.0        | -91         | 0.0  | 0.0        | -184        | 0.4  | 2.1        | 41        | <b>0.4</b>   | <b>5.4</b> | <b>102</b> | 0.2  | 3.3        | 133        | <b>0.3</b>   | <b>4.5</b> | <b>316</b> | 0.6  | 2.0        | 40        | <b>0.4</b>   | <b>4.5</b> | <b>96</b> | 0.3  | 2.7        | 123        | 0.2  | 4.1        | 307        |  |
| SRPI                     | 0.4   | 0.0        | -58        | 0.2   | 0.1        | -48        | 0.0   | 0.0        | -91         | 0.0  | 0.0        | -184        | 0.4  | 2.2        | 42        | 0.4  | 5.5        | 102        | 0.2  | 3.3        | 133        | 0.3  | 4.6        | 318        | 0.5  | 2.1        | 41        | 0.4  | 4.6        | 96        | 0.3  | 2.7        | 123        | 0.1  | 4.2        | 308        |  |
| <i>Exponential model</i> |   |            |            |   |            |            |   |            |             |  |            |             |  |            |           |  |            |            |  |            |            |  |            |            |  |            |           |  |            |           |  |            |            |  |            |            |  |
| SR                       | 0.8   | 0.0        | -69        | 0.4   | 0.0        | -53        | 0.4   | 0.0        | -103        | 0.2  | 0.0        | -193        | 0.9  | 0.9        | 26        | 0.1  | 6.2        | 106        | 0.5  | 2.7        | 122        | 0.2  | 4.8        | 325        | 0.9  | 1.1        | 28        | 0.1  | 5.6        | 102       | 0.4  | 2.5        | 118        | 0.2  | 4.0        | 305        |  |
| GRI                      | 0.4   | 0.0        | -58        | <b>0.5</b>  | <b>0.0</b> | <b>-57</b> | 0.5   | 0.0        | -106        | <b>0.4</b>   | <b>0.0</b> | <b>-208</b> | 0.7  | 1.5        | 35        | 0.1  | 6.2        | 106        | 0.5  | 2.7        | 122        | 0.1  | 5.2        | 333        | 0.8  | 1.3        | 32        | 0.1  | 5.6        | 102       | 0.4  | 2.6        | 121        | 0.1  | 4.2        | 310        |  |
| WI                       | 0.6   | 0.0        | -62        | 0.2   | 0.1        | -47        | 0.4   | 0.0        | -105        | 0.2  | 0.0        | -194        | <b>0.9</b>   | <b>0.8</b> | <b>24</b> | 0.0  | 6.3        | 106        | 0.4  | 3.1        | 129        | 0.1  | 5.1        | 331        | 0.9  | 1.2        | 30        | 0.0  | 5.8        | 104       | 0.3  | 2.8        | 124        | 0.1  | 4.2        | 311        |  |
| NDVI                     | 0.7   | 0.0        | -66        | 0.4   | 0.0        | -52        | 0.5   | 0.0        | -108        | 0.2  | 0.0        | -198        | 0.9  | 1.1        | 29        | 0.1  | 6.1        | 105        | 0.6  | 2.5        | 120        | 0.3  | 4.7        | 322        | 0.9  | 0.7        | 22        | 0.1  | 5.5        | 102       | 0.5  | 2.4        | 117        | 0.2  | 3.9        | 303        |  |
| SIPI                     | 0.6   | 0.0        | -62        | 0.3   | 0.0        | -51        | <b>0.5</b>  | <b>0.0</b> | <b>-109</b> | 0.2  | 0.0        | -195        | 0.7  | 1.6        | 35        | 0.2  | 5.9        | 104        | 0.6  | 2.5        | 118        | <b>0.3</b>   | <b>4.4</b> | <b>315</b> | 0.8  | 1.2        | 31        | 0.2  | 5.2        | 100       | 0.5  | 2.3        | 114        | <b>0.3</b>   | <b>3.8</b> | <b>300</b> |  |
| CI                       | 0.6   | 0.0        | -63        | 0.4   | 0.0        | -53        | 0.5   | 0.0        | -106        | 0.2  | 0.0        | -199        | 0.9  | 1.0        | 28        | 0.2  | 5.9        | 104        | <b>0.6</b>   | <b>2.3</b> | <b>115</b> | 0.2  | 4.7        | 324        | <b>1.0</b>   | <b>0.6</b> | <b>18</b> | 0.2  | 5.3        | 101       | <b>0.6</b>   | <b>2.2</b> | <b>111</b> | 0.3  | 3.9        | 302        |  |
| PRI                      | <b>0.8</b>  | <b>0.0</b> | <b>-71</b> | 0.2   | 0.1        | -48        | 0.0   | 0.0        | -91         | 0.0  | 0.0        | -185        | 0.7  | 1.5        | 35        | 0.2  | 5.9        | 104        | 0.2  | 3.4        | 134        | 0.3  | 4.6        | 319        | 0.7  | 1.6        | 36        | 0.2  | 5.4        | 101       | 0.2  | 3.0        | 128        | 0.1  | 4.2        | 311        |  |
| EVI                      | 0.8   | 0.0        | -68        | 0.4   | 0.0        | -54        | 0.5   | 0.0        | -109        | 0.2  | 0.0        | -198        | 0.8  | 1.2        | 31        | 0.1  | 6.1        | 105        | 0.4  | 2.8        | 125        | 0.2  | 4.8        | 325        | 0.9  | 1.0        | 27        | 0.1  | 5.5        | 102       | 0.4  | 2.6        | 121        | 0.2  | 4.1        | 308        |  |
| NPQI                     | 0.0   | 0.0        | -54        | 0.0   | 0.1        | -45        | 0.4   | 0.0        | -104        | 0.1  | 0.0        | -192        | 0.2  | 2.5        | 44        | 0.1  | 6.3        | 106        | 0.1  | 3.6        | 137        | 0.1  | 5.2        | 333        | 0.2  | 2.7        | 45        | 0.1  | 5.6        | 103       | 0.1  | 3.2        | 130        | 0.0  | 4.5        | 318        |  |
| NPCI                     | 0.4   | 0.0        | -58        | 0.2   | 0.0        | -49        | 0.0   | 0.0        | -91         | 0.0  | 0.0        | -184        | 0.4  | 2.3        | 43        | <b>0.3</b>   | <b>5.5</b> | <b>102</b> | 0.2  | 3.4        | 133        | 0.3  | 4.5        | 319        | 0.4  | 2.3        | 42        | <b>0.3</b>   | <b>4.8</b> | <b>98</b> | 0.3  | 2.8        | 124        | 0.2  | 4.1        | 309        |  |
| SRPI                     | 0.3   | 0.0        | -58        | 0.2   | 0.0        | -49        | 0.0   | 0.0        | -91         | 0.0  | 0.0        | -184        | 0.3  | 2.4        | 43        | 0.3  | 5.6        | 103        | 0.2  | 3.4        | 134        | 0.3  | 4.6        | 320        | 0.4  | 2.4        | 43        | 0.3  | 4.9        | 98        | 0.3  | 2.8        | 124        | 0.1  | 4.2        | 310        |  |